Effect the orientation of porous silicon on solar cells performance

W. J. AZIZ*, A. RAMIZY, K. IBRAHIM, K. OMAR, Z. HASSAN
Nano-Optoelectronics Research and Technology Laboratory, School of Physics, Universiti Sains Malaysia, 11800 USM, Penang, Malaysia

The solar cells have been fabricated based on porous silicon with N (111) and N (100) which prepared by electrochemical etching with an electrolyte solution HF: ethanol in the ratio of 1:3 Surface morphology and structural properties of nanostructures were characterized by using scanning electron microscopy (SEM) .Optical reflectance was obtained by using optical reflectometer. I-V characterizations were studied with 80 mW/cm^2 illumination conditions. Porous silicon N(100) revealed as excellent anti-reflection coating versus incident light when it is compare to porous silicon N(111) anti-reflection coating as well as it is given a good light-trapping of wide wavelength spectrum, which could be produced a high efficiency solar cells.

(Received November 17, 2009; accepted November 23, 2009)

Keywords: Porous silicon, Solar cells, High efficiency, Doping type, Orientation

1. Introduction

Porous silicon (PS) is an efficient light emitting system, most efficient than many III-V semiconductor systems [1]. However, size reduction to a few nanometers is needed to observe a strong visible light emission. Porous silicon (PS) has been considered an important candidate for silicon-based applications such as light emitting, light sensing devices due to its remarkable luminescence properties [2-3]. This properties make the porous silicon very attractive for solar cell applications include band gap broadening, wide absorption spectrum, wide optical transmission range (700–1000 nm), and good antireflection (AR) coating for Si solar cells. Porous silicon also can be used for surface passivation and texturisation [4-9].

The electrochemical process considered a promising technique to fabricate PS [10-13]. According to the quantum confinement model, a hetero-junction have formed between Si substrate and porous layer due to the band gap of porous layer, which is bigger than bulk (1.7–2.2 eV) [14].

On etched surface, the H-passivation is highest on silicon (111) than on (100) oriented, which has the lowest possible value due to the number of dangling bonds which have to be significantly higher on (100) than on (111) orientation of crystalline [15].

2. Experimental procedure

The porous silicon was fabricated by electrochemical etching of N-type silicon wafers with (111) and (100) orientation, resistivity of 0.75 $\Omega.cm$, thickness 287 μm. The solar cells have been fabricated based on porous silicon which prepared with an electrolyte solution HF: ethanol, 1:3 ml, time duration is 20 minutes and current density has set at 50 mA/cm^2. Before etching process, silicon (Si) substrate was cleaned to remove the oxide layer by the RCA method. Si wafer was immersed in HF acid to remove the native oxide. The electrochemical cell was made of teflon and has a circular aperture on its bottom, under which the silicon wafer is sealed. The cell was a two-electrode system with a silicon wafer as anode and platinum as cathode. The synthesis was carried out at room temperature. After etching processing all samples were rinsed with ethanol and dried in air. Surface morphology and structural properties of nanostructures were characterized by using scanning electron microscopy (SEM). Photoluminescence (PL) and Raman spectroscopy measurements was also performed at room temperature by using He-Cd laser ($\lambda = 325nm$) and ion-argon laser ($\lambda = 514nm$) respectively. P-type doping was achieved using boron dopant. Aluminum was used for back metal contact and for front metallization, silver was used. Contact annealing is done at 400C^0 for 20 min. The device was characterized using current-voltage (I-V) measurement. Optical reflectance was obtained using optical reflectometer (Filmetrics F20).

3. Results and discussion

The SEM images in Figs. 1 and 2 obtain the grains of the surface texturing which have similar grain geometry. This is due to the isotropic character of the HF/HNO_3 etching and the optimal conditions for current density and etching time. Moreover, the area of surface has been observed in the SEM image of all the surfaces that are etched.

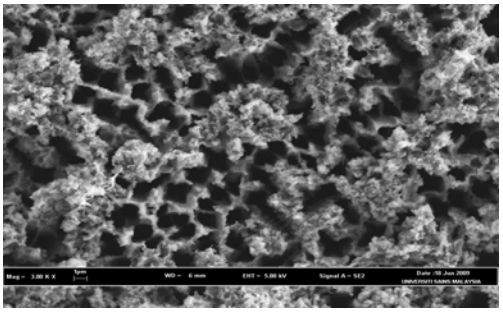

Fig. 1. SEM image of porous silicon N(100).

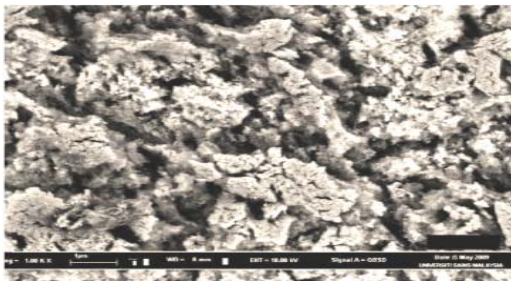

Fig. 2. SEM image of porous silicon P(100).

The surface reflections of porous silicon N (100) shows a reduction of incoming light reflection and increasing in light capturing of wide wavelength range compared with porous silicon N (111) reflection as illustrate in Fig. 3 which due to (100) surface formed to be preferentially dissolved and preferred pore tips but (111) surface is most effectively to preferred pore walls at etching processing. Fig. 4 reveals Raman spectra of bulk silicon, which show a sharp line in the spectra with (FWHM) of 3.5 cm^{-1} shifted by 522 cm^{-1} relative to the laser line incident. On other hand, porous silicon spectra is broadened relative to the 517 cm^{-1} sharp with (FWHM) of 8.2 cm^{-1} in porous silicon N(111) and shifted to 510 cm^{-1} with (FWHM) of 17.3 cm^{-1} in porous silicon N(100) which is attributed to the quantum confinement of optical phonons.

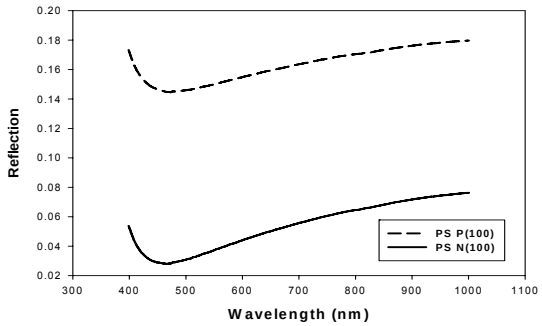

Fig. 3. The reflectance spectra for porous silicon N(100) and P(100).

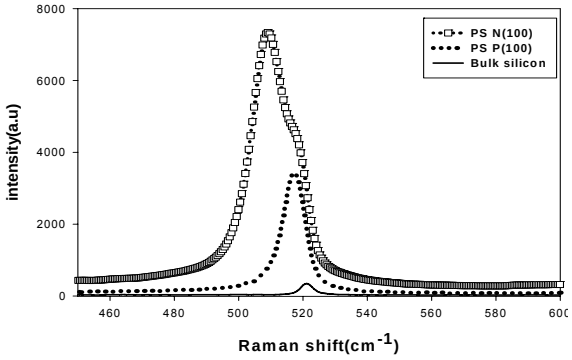

Fig. 4. Raman spectra of porous silicon prepared by electrochemical etching.

Fig. 5 shows the PL spectrum of porous silicon N(111) at 699 nm (1.77 eV) with a full-width and half maximum (FWHM) of about 135 nm. In porous silicon N(100) observe the photoluminescence at 680 nm (1.82 eV) with a full-width and half maximum (FWHM) of about 142 nm. This means that the particles are confined into lower dimension and this will lead to a higher efficiency.

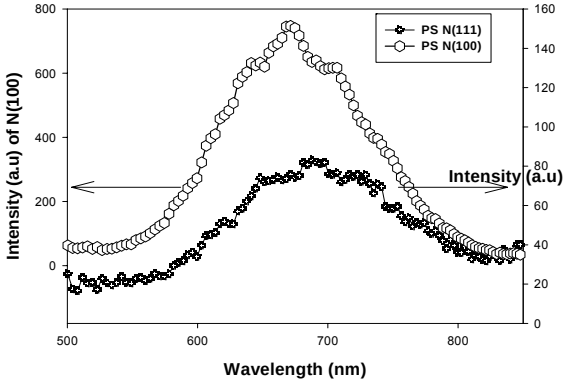

Fig. 5. PL spectra of porous silicon prepared by electrochemical etching.

The experimental data in Fig. 6 and Table 1 shows that solar cell with porous silicon N(100) increase the short-circuit current from 12.4 to 15.85 mA/cm2, open current voltage from 0.44 to 0.48 and conversation efficiency from 11.23 to 15.42.

Table 1. Fill factor (FF) and efficiency (η) of porous silicon N(100) and P(100).

Samples	V_m (V)	I_m (mA)	V_{oc} (V)	I_{sc} (mA)	FF	Efficiency (η)
PS N(111)	0.36	12.39	0.44	12.4	0.82	11.23%
PS N(100)	0.41	15.12	0.48	15.85	0.81	15.42%

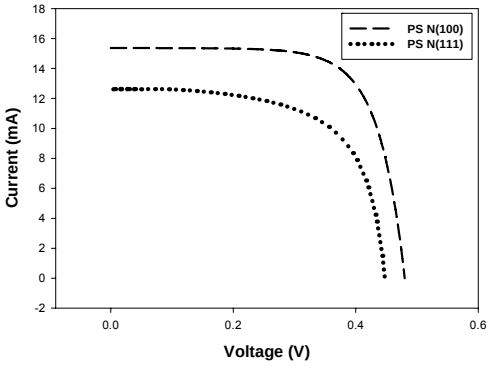

Fig. 6. Current-voltage characteristics of porous silicon N(100) and P(100) solar cells.

Sundaram reported that the etching rate of the (100) and (110) crystallographic planes increased faster than the etching rate of the (111) crystallographic plane [16].

4. Conclusions

The selection of orientation type (111) or (100) of the silicon wafers allows controlling the local current density as well as the driving force for the separation phase. The oxidizing component which is existent in (100) more than in (111) produce to dissolved and formed the (100) surface as pore tips which results in higher pyramids, lower reflectance and high efficiency solar cell in N (100). The H-passivation is higher on (111) than the (100) surfaces for this the time scale which depends on the time of dissolving oxide will be in (111) more than in (100) and lead to formed the (111) surface as pore walls. For these reasons the selectivity between (100) and (111) surfaces will exist which is essential for stable pore growth with small size and size distribution.

The experimental results showed that solar cells with porous silicon N(100) had increased conversation efficiency from 11.23 to 15.42.

References

[1] L.T. Canham, Appl. Phys. Lett. **57**, 1046 (1990).
[2] A. G. Cullis, L. T. Canham, P. D. J. Calcott, J. Appl. Phys. **82,** 909 (1997).
[3] S. N. Sharma, R. Banerjee, D. Das, S. Chattopadhyay, A. K. Barua, Appl. Surf. Sci. **182,** 333 (2001) .
[4] P. Menna, G. D. Francia, V. L. Ferrara, Solar Energy Mat. & Solar Cells **37,** 13 (1997).
[5] L. Schirone, G. Sotgiu, M. Montecchi, A. Parisini, Proc. 14111 European PV Solar Energy Conf. 1479, 1997.
[6] L. Schirone, G. Sotgiu, M. Montecchi, G. Righini, R. Zanoni, Proc. 2"d World Conf. PV Solar Energy Conversion, 276, 1998.
[7] V. Yerokhov, I. Mclnyk, Renewable and Sustainable Energy Reviews **3,** 291 (1999).
[8] P. Menna, G. Di Francia, V. La Ferrara, Solar Energy Materials and Solar Cells **37,** 12 (1995).
[9] R. Cláudia, B. Miranda, M. R. Baldan, A. F. Beloto, N. G. Ferreira, J. Braz. Chem. Soc. **19**, 769 (2008).
[10] D. Hyun Oha, B. T. Whan Kima, W. Jo Chob, K. Dal Kwacka, J. of Ceramic Processing Research. **9,** 57 (2008).
[11] G. Barillaro, A. Nannini, F. Pieri, J. Electrochem. Soc. **149,** 180 (2002).
[12] G. Jia, Winfried Seifert, T. Arguirov, M. Kittler, J. Mater. Sci.: Mater Electron. **19,** 509 (2008).
[13] F. Yan, X. Bao, T. Gao, Solid State Commun. **91,** 341 (1994).
[14] M. Yamaguchi, Super-high efficiency III-V tandem and multijunction cells, M. Archer, and R. Hill, World Scientific Publishing, Singapore, 347, 2001.
[15] S. Rönnebeck, S. Ottow, J. Carstensen, H. Föll, J. Electrochem. Soc. Lett. **2,** 126 (1999).
[16] B. Sundaram k, A.Vijayakumar, G. Subramanian, Micro. Eng. **77,** 230 (2005).

*Corresponding author: wisam_jafer@yahoo.com